A Bound for the Magnitude Characteristics of Nonlinear Output Frequency Response Functions

Part I: Analysis and Computation

S A Billings and Zi-Qiang Lang
Department of Automatic Control and Systems Engineering
University of Sheffield
Mappin Street
Sheffield
S1 3JD
UK

Research Report No 571

April 1995

A BOUND FOR THE MAGNITUDE CHARACTERISTICS OF NONLINEAR OUTPUT FREQUENCY RESPONSE FUNCTIONS
PART I: ANALYSIS AND COMPUTATION

S.A. Billings and Zi-Qiang Lang

Department of Automatic Control and Systems Engineering
University of Sheffield, Mappin Street
Sheffield, S1 3JD, U.K.

Abstract: A bound for the magnitude frequency domain characteristics associated with the outputs of a wide class of nonlinear systems is derived as a relatively simple function of the generalised frequency response functions and properties of the system inputs. It is shown how the practical computation of the new bound can be easily performed for nonlinear systems with finite but arbitrary order nonlinearities and worked examples are included. The paper is divided into two parts. In Part I, an expression for the output magnitude bound is derived, properties of the result are discussed and general procedures for the practical computation of the bound are developed. In Part II the practical computations associated with applying the bound to the polynomial NARX model (Nonlinear AutoRegressive model with eXogenous input) are discussed.

1. INTRODUCTION

The frequency domain analysis of nonlinear systems has to date been largely based upon the generalised frequency response functions (GFRFs) which represent the nonlinear frequency response behaviour in the form of multidimensional transfer functions which are independent of the input. The estimation and analysis of the GFRFs have been studied by several authors (Bedrosian and Rice 1971, Bussgang et al. 1974, Vinh et al. 1987, Kim and Powers 1988, Billings and Tsang 1989(a) and 1989(b), Peyton Jones and Billings 1989, Billings , Tsang and Tomlinson 1990, Billings and Peyton Jones 1990, Cho, et al. 1992, Zhang, Billings and Zhu 1993) and important properties and characteristics of practical nonlinear systems have been investigated based on a graphical interpretation of these functions (Powers and Miksad 1987, Worden et al. 1993 , Billings and Yusof 1994).

But analysis in the frequency domain usually involves two other problems which are often referred to as the analysis and synthesis problems. The analysis problem involves determining how the output frequency response is determined as a function of the frequency characteristics of the input and the frequency domain properties of the system. The synthesis problem consists of determining the frequency domain characteristics of the system in order to obtain a satisfactory output frequency response for a given input excitation. Solutions to both these problems rely on the analysis of the relationship between the frequency characteristics of the system input and output. These problems are well known and solutions exist for linear systems but few results are available when the system is nonlinear. Extension of the linear results to the nonlinear case is far from straightforward and in the present study this problem is partially solved by deriving a new expression for the bound on the output magnitude frequency domain characteristics of a wide class of nonlinear systems. The results reveal how the effect of the GFRFs and the input characteristics can be analysed as separate influences on the system output frequency domain properties. Practical computations based on the new frequency domain output magnitude bound can easily be performed using the methods developed in this paper for nonlinear systems with finite but arbitrary order nonlinearities. This new concept provides a basis for the analysis and synthesis of nonlinear systems in the frequency domain and provides valuable information for studies which involve truncation of nonlinear system expansions.

The paper is divided into two parts. The new bound on the output magnitude expression in the frequency domain is derived in Part I together with general aspects relating to the practical computation and two simple examples. Part II is focused on the practical computation of the bound for the polynomial NARX model (Nonlinear AutoRegresive model with eXogenous input).

2. THE SYSTEM INPUT AND OUTPUT DESCRIPTIONS IN THE FREQUENCY DOMAIN

For a linear system it is well known that the output frequency response can be related to the corresponding input frequency characteristic by the simple linear relationship

$$\mathbf{Y}(j\omega) = H(j\omega)U(j\omega) \tag{2.1}$$

where $\mathbf{Y}(j\omega)$ and $U(j\omega)$ represent the Fourier transforms of the output and input and $H(j\omega)$ is the system frequency response function.

For nonlinear systems which are stable at the zero equilibrium point and can be described in the neighbourhood of the equilibrium point by the Volterra series

$$y(t) = \sum_{n=1}^{N} \int_{-\infty}^{\infty} \cdots \int_{-\infty}^{\infty} h_n(\tau_1, \ldots, \tau_n) \prod_{i=1}^{n} u(t-\tau_i) d\tau_i \tag{2.2}$$

where $y(t)$ and $u(t)$ represent the system output and input respectively and $h_n(\tau_1,\ldots,\tau_n)$ is the nth order Volterra kernel, the extension of the linear frequency domain description (2.1) can be obtained as (Lang and Billings 1994)

$$\begin{cases} \mathbf{Y}(j\omega) = \sum_{n=1}^{N} Y_n(j\omega) \quad \text{for } \forall\omega \\ Y_n(j\omega) = \dfrac{1/\sqrt{n}}{(2\pi)^{n-1}} \displaystyle\int_{\omega_1+,\ldots,+\omega_n=\omega} Y_n(j\omega_1, \ldots, j\omega_n) d\sigma_\omega \\ Y_n(j\omega_1, \ldots, j\omega_n) = H_n(j\omega_1, \ldots, j\omega_n) \prod_{i=1}^{n} U(j\omega_i) \end{cases} \tag{2.3}$$

when the system is excited by the general input

$$u(t) = U_0 + \tfrac{1}{2\pi} \int_0^{\infty} 2|U(j\omega)| \cos[\omega t + \angle U(j\omega)] d\omega = \tfrac{1}{2\pi} \int_{-\infty}^{\infty} U(j\omega) e^{j\omega t} d\omega \tag{2.4}$$

where $U_0 = \tfrac{1}{2\pi} U(0)$. In (2.3) $Y_n(j\omega)$ represents nth order output frequency characteristic, and

$$H_n(j\omega_1,\ldots,j\omega_n) = \int_{-\infty}^{\infty}\cdots\int_{-\infty}^{\infty} h(\tau_1,\ldots,\tau_n)e^{-(\omega_1\tau_1+,\ldots,+\omega_n\tau_n)}d\tau_1\cdots d\tau_n \tag{2.5}$$

is known as the nth order generalised frequency response function of the system, and $\int_{\omega_1+,\ldots,+\omega_n=\omega} Y_n(j\omega_1,\ldots,j\omega_n)d\sigma_\omega$ denotes the integration of $Y_n(j\omega_1,\ldots,j\omega_n)$ over the n-dimensional hyperplane $\omega = \omega_1+,\ldots,+\omega_n$.

The output frequency response of a system contains the information about both the magnitude and phase. But the magnitude information is often considered to be more important because according to Parseval's theorem the energy of the system output can be completely represented by the magnitude characteristic of the output frequency response. From (2.1) , the magnitude characteristic of $\mathbf{Y}(j\omega)$ can be obtained as

$$|\mathbf{Y}(j\omega)| = |H(j\omega)||U(j\omega)| \tag{2.6}$$

which is an important basis of most analysis and synthesis methods for linear systems in the frequency domain. From (2.3) the extension of (2.6) to the nonlinear case is given as

$$|\mathbf{Y}(j\omega)| = \left|\sum_{n=1}^{N} \frac{1/\sqrt{n}}{(2\pi)^{n-1}} \int_{\omega_1+,\ldots,+\omega_n=\omega} H_n(j\omega_1,\ldots,j\omega_n)\prod_{i=1}^{n} U(j\omega_i)d\sigma_\omega\right| \tag{2.7}$$

Because of the complexity of (2.7) this is generally very difficult to analyse. In order to resolve this problem the concept of a bound for $|\mathbf{Y}(j\omega)|$ in (2.7) is proposed in the next section and an expression is derived which has a form similar to (2.6) in the sense that the effects of the GFRFs and $U(j\omega)$ on this bound are decomposed for each term in the expression.

3. EXPRESSION FOR THE BOUND ON THE OUTPUT MAGNITUDE FREQUENCY DOMAIN CHARACTERISTICS OF NONLINEAR SYSTEMS

Consider a nonlinear system excited by the general input and expressed in the frequency domain by (2.3). From the first and second equation in (2.3) it is obvious that

$$|\mathbf{Y}(j\omega)| \le \sum_{n=1}^{N} |Y_n(j\omega)| \le \sum_{n=1}^{N} \frac{1/\sqrt{n}}{(2\pi)^{n-1}} \int_{\omega_1+,\ldots,+\omega_n=\omega} |Y_n(j\omega_1,\ldots,j\omega_n)|d\sigma_\omega = \sum_{n=1}^{N} Y_n^B(\omega) \tag{3.1}$$

where

$$Y_n^B(\omega) = \frac{1/\sqrt{n}}{(2\pi)^{n-1}} \int_{\omega_1+,\ldots,+\omega_n=\omega} |Y_n(j\omega_1,\ldots,j\omega_n)|d\sigma_\omega \tag{3.2}$$

Define

$$\mathbf{Y}^B(\omega) = \sum_{n=1}^{N} Y_n^B(\omega) \tag{3.3}$$

which is clearly a bound for the magnitude characteristic of the system output frequency response.

Substituting the third equation from (2.3) into (3.2) yields

$$Y_n^B(\omega) = \frac{1/\sqrt{n}}{(2\pi)^{n-1}} \int_{\omega_1+,\ldots,+\omega_n=\omega} \left| H_n(j\omega_1,\ldots,j\omega_n) \prod_{i=1}^{n} U(j\omega_i) \right| d\sigma_\omega \quad (3.4)$$

For the simplest case of n=1 in (3.4),

$$Y_n^B(\omega) = Y_1^B(\omega) = \frac{1}{(2\pi)^0} |H_1(j\omega)||U(j\omega)| = |Y_1(j\omega)| \quad (3.5)$$

indicating that if N=1 then the bound for the magnitude frequency response of the system and the response itself are identical.

For the case of n=2, (3.4) can be written as

$$Y_2^B(\omega) = \frac{1/\sqrt{2}}{(2\pi)^{2-1}} \int_{\omega_1+\omega_2=\omega} \left| H_2(j\omega_1, j\omega_2) \prod_{i=1}^{2} U(j\omega_i) \right| d\sigma_\omega \quad (3.6)$$

Considering that in Calculus the integration of a function $f(x_1, x_2)$ over a two dimensional curved line S: $x_2 = x_2(x_1)$ can be expressed and calculated using (Spiegel 1971)

$$\int_S f(x_1,x_2) d\sigma_S = \int_{S_{x_1}} f[x_1, x_2(x_1)] \sqrt{1 + \left(\frac{\partial x_2}{\partial x_1}\right)^2} dx_1 \quad (3.7)$$

where $d\sigma_s$ represents the length of a minute line segment on S and S_{x_1} represents the projection of S onto the axis $x_2 = 0$, (3.6) can be further expressed as

$$\begin{aligned} Y_2^B(\omega) &= \frac{1/\sqrt{2}}{(2\pi)^{2-1}} \int_{S_{\omega_1}} |H_2[j\omega_1, j(\omega-\omega_1)]||U(j\omega_1)||U[j(\omega-\omega_1)]| \sqrt{2} d\omega_1 \\ &= \frac{1}{(2\pi)} \int_{S_{\omega_1}} |H_2[j\omega_1, j(\omega-\omega_1)]||U(j\omega_1)||U[j(\omega-\omega_1)]| d\omega_1 \end{aligned} \quad (3.8)$$

where S_{ω_1} denotes the projection of $\omega_1 + \omega_2 = \omega$ onto the axis $\omega_2 = 0$. Assume that the input frequency characteristic $U(j\omega)$ satisfies the following relationship

$$\begin{cases} |U(j\omega)| \neq 0 & \text{when } |\omega| \leq b \\ |U(j\omega)| = 0 & \text{otherwise} \end{cases} \quad (3.9)$$

The integration area for the case n=2 can then be illustrated as shown in Fig.1 and

$$\begin{aligned} Y_2^B(\omega) &= \frac{1/\sqrt{2}}{(2\pi)} \int_{\overline{AB}} |H_2(j\omega_1, \omega_2)| \prod_{i=1}^{2} |U(j\omega_i)| d\sigma_{\overline{AB}} \\ &= \frac{1}{(2\pi)} \int_{\overline{\omega_{1A}\omega_{1B}}} |H_2[j\omega_1, j(\omega-\omega_1)]||U(j\omega_1)||U[j(\omega-\omega_1)]| d\omega_1 \end{aligned}$$

$$=\frac{1}{(2\pi)}\int_{\omega_{1A}}^{\omega_{1B}}|H_2[j\omega_1, j(\omega-\omega_1)]||U(j\omega_1)||U[j(\omega-\omega_1)]|d\omega_1 \tag{3.10}$$

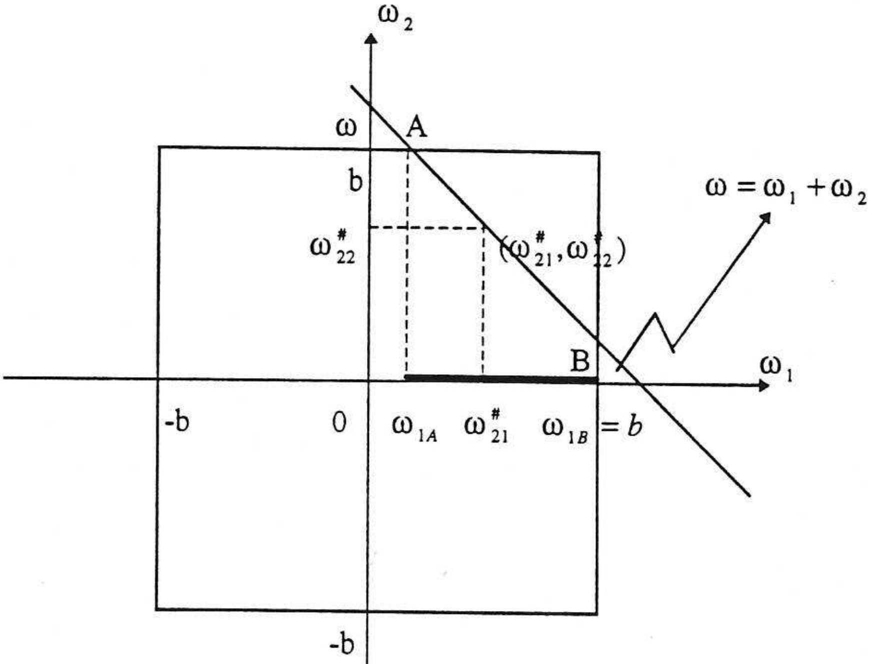

Fig.1. Illustration of the integration area for the case of n=2

In integration theory, it is well known from one of the theorems of mean value (James and James, 1959) that if a function $g(x)$ is continuous and $f(x)$ is integrable and does not change sign in the interval $c \le x \le d$, then

$$\int_c^d f(x)g(x)dx = g(\xi)\int_c^d f(x)dx \tag{3.11}$$

where $c \le \xi \le d$.

Applying this theorem to (3.10) with

$$f = |U(j\omega_1)||U[j(\omega-\omega_1)]| \tag{3.12}$$

and

$$g = |H_2[j\omega_1, j(\omega-\omega_1)]| \tag{3.13}$$

yields

$$Y_2^B(\omega) = \frac{1}{(2\pi)}|H_2[j\omega_{21}^\#, j(\omega-\omega_{21}^\#)]|\int_{\omega_{1A}}^{\omega_{1B}}|U(j\omega_1)||U[j(\omega-\omega_1)]|d\omega_1$$

$$=\frac{1}{(2\pi)}|H_2[j\omega_{21}^\#, j(\omega-\omega_{21}^\#)]|\int_{-\infty}^{\infty}|U(j\omega_1)||U[j(\omega-\omega_1)]|d\omega_1$$

$$=\frac{1}{(2\pi)}|H_2[j\omega_{21}^\#, j\omega_{22}^\#)]||U|*|U(j\omega)| \tag{3.14}$$

where $|U| * |U(j\omega)| = \int_{-\infty}^{\infty} |U(j\omega_1)||U[j(\omega - \omega_1)]| d\omega_1$, $\omega_{21}^{\#} \in [\omega_{1A}, \omega_{1B}]$, $\omega_{22}^{\#} = \omega - \omega_{21}^{\#}$, and as shown in Fig.1 $(\omega_{21}^{\#}, \omega_{22}^{\#})$ is a point on the straight line $\omega_1 + \omega_2 = \omega$ between the two points A and B.

For n=3 in (3.4),

$$Y_3^B(\omega) = \frac{1/\sqrt{3}}{(2\pi)^2} \int_{\omega_1+\omega_2+\omega_3=\omega} \left| H_3(j\omega_1, \omega_2, j\omega_3) \prod_{i=1}^{3} U(j\omega_i) \right| d\sigma_\omega$$

$$= \frac{1/\sqrt{3}}{(2\pi)^2} \int_{S_{\omega_1\omega_2}} |H_3[j\omega_1, j\omega_2, j(\omega - \omega_1 - \omega_2)]||U(j\omega_1)||U(j\omega_2)||U[j(\omega - \omega_1 - \omega_2)]|$$

$$\sqrt{1 + \left[\frac{\partial(\omega - \omega_1 - \omega_2)}{\partial\omega_1}\right]^2 + \left[\frac{\partial(\omega - \omega_1 - \omega_2)}{\partial\omega_2}\right]^2} \, d\omega_1 d\omega_2$$

$$= \frac{1}{(2\pi)^2} \int_{S_{\omega_1\omega_2}} |H_3[j\omega_1, j\omega_2, j(\omega - \omega_1 - \omega_2)]||U(j\omega_1)||U(j\omega_2)||U[j(\omega - \omega_1 - \omega_2)]| d\omega_1 d\omega_2 \tag{3.15}$$

where $S_{\omega_1\omega_2}$ represents the projection of $\omega_1 + \omega_2 + \omega_3 = \omega$ onto the plane $\omega_3 = 0$. Under the assumption for $U(j\omega)$ given in (3.9) and illustrated in Fig.2 equation (3.15) can be written as

$$Y_3^B(\omega) = \frac{1}{(2\pi)^2} \int_{\omega_1^1}^{\omega_1^2} \int_{\omega_2^1(\omega_1)}^{\omega_2^2(\omega_1)} |H_3[j\omega_1, j\omega_2, j(\omega - \omega_1 - \omega_2)]| \; |U(j\omega_1)||U(j\omega_2)||U[j(\omega - \omega_1 - \omega_2)]| d\omega_1 d\omega_2 \tag{3.16}$$

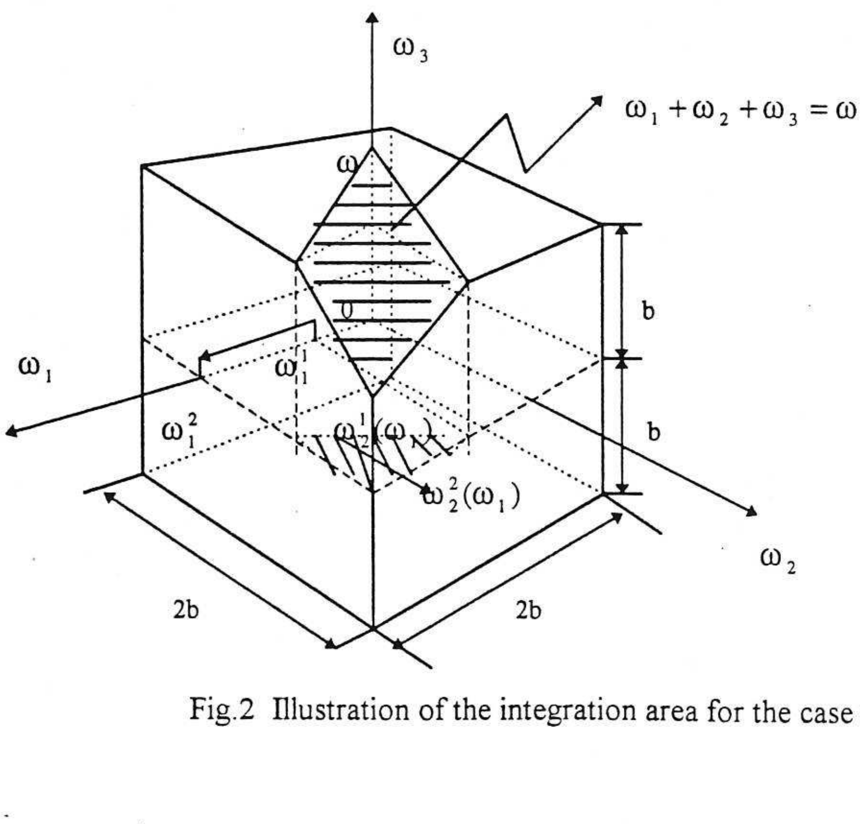

Fig.2 Illustration of the integration area for the case of n=3

Applying the theorem of mean value to the integration for ω_2 in (3.16) with

$$f = |U(j\omega_1)||U(j\omega_2)||U[j(\omega-\omega_1-\omega_2)]| \tag{3.17}$$

$$g = |H_3[j\omega_1, j\omega_2, j(\omega-\omega_1-\omega_2)]| \tag{3.18}$$

yields

$$Y_3^B(\omega) = \frac{1}{(2\pi)^2}\int_{\omega_1^1}^{\omega_1^2} |H_3[j\omega_1, j\omega_2'(\omega_1), j(\omega-\omega_1-\omega_2'(\omega_1))]| \int_{\omega_2^1(\omega_1)}^{\omega_2^2(\omega_1)} |U(j\omega_1)||U(j\omega_2)||U[j(\omega-\omega_1-\omega_2)]| d\omega_1 d\omega_2 \tag{3.19}$$

where $\omega_2'(\omega_1)$ is a function of ω_1 and satisfies

$$\omega_2^1(\omega_1) \le \omega_2'(\omega_1) \le \omega_2^2(\omega_1) \tag{3.20}$$

Applying the theorem of mean value again to (3.19) but with

$$f = \int_{\omega_2^1(\omega_1)}^{\omega_2^2(\omega_1)} |U(j\omega_1)||U(j\omega_2)||U[j(\omega-\omega_1-\omega_2)]| d\omega_2, \tag{3.21}$$

$$g = |H_3[j\omega_1, j\omega_2'(\omega_1), j(\omega-\omega_1-\omega_2'(\omega_1))]|, \tag{3.22}$$

gives

$$Y_3^B(\omega) = \frac{1}{(2\pi)^2} |H_3[j\omega_1', j\omega_2'(\omega_1'), j(\omega-\omega_1'-\omega_2'(\omega_1'))]| \int_{\omega_1^1}^{\omega_1^2}\int_{\omega_2^1(\omega_1)}^{\omega_2^2(\omega_1)} |U(j\omega_1)||U(j\omega_2)||U[j(\omega-\omega_1-\omega_2)]| d\omega_1 d\omega_2 \tag{3.23}$$

where $\omega_1^1 \le \omega_1' \le \omega_1^2$. Denoting

$$\omega_1' = \omega_{31}^\#,\quad \omega_2'(\omega_1') = \omega_{32}^\#,\quad \text{and } \omega - \omega_1' - \omega_2'(\omega_1') = \omega_{33}^\#$$

in (3.23) yields

$$Y_3^B(\omega) = \frac{1}{(2\pi)^2} |H_3[j\omega_{31}^\#, j\omega_{32}^\#, j\omega_{33}^\#]| \int_{\omega_1^1}^{\omega_1^2}\int_{\omega_2^1(\omega_1)}^{\omega_2^2(\omega_1)} |U(j\omega_1)||U(j\omega_2)||U[j(\omega-\omega_1-\omega_2)]| d\omega_1 d\omega_2$$

$$= \frac{1}{(2\pi)^2} |H_3[j\omega_{31}^\#, j\omega_{32}^\#, j\omega_{33}^\#]| \int_{-\infty}^{\infty}\int_{-\infty}^{\infty} |U(j\omega_1)||U(j\omega_2)||U[j(\omega-\omega_1-\omega_2)]| d\omega_1 d\omega_2$$

$$= \frac{1}{(2\pi)^2} |H_3[j\omega_{31}^\#, j\omega_{32}^\#, j\omega_{33}^\#]| |U| * |U| * |U(j\omega)| \tag{3.24}$$

where

$$|U| * |U| * |U(j\omega)| = \int_{-\infty}^{\infty}\int_{-\infty}^{\infty} |U(j\omega_1)||U(j\omega_2)||U[j(\omega-\omega_1-\omega_2)]| d\omega_1 d\omega_2$$

It is worth noting that for clarity of derivation only simple situations are considered above. For more complicated cases, such as the case

$$\begin{cases} |U(j\omega)| \neq 0 & \text{when } 0 < a \le |\omega| \le b, \\ |U(j\omega)| = 0 & \text{otherwise} \end{cases} \tag{3.25}$$

for example, (3.14) and (3.24) can also be proved using similar ideas.

Extending (3.5), (3.14) and (3.24) to arbitrary order nonlinearities yields

$$Y_n^B(\omega) = \frac{1}{(2\pi)^{n-1}} |H_n[j\omega_{n1}^{\#}, j\omega_{n2}^{\#}, \ldots, j\omega_{nn}^{\#}]| \underbrace{|U| * |U| * \ldots * |U(j\omega)|}_{n} \tag{3.26}$$

where $\{\omega_{n1}^{\#}, \omega_{n2}^{\#}, \ldots, \omega_{nn}^{\#}\}$ denotes the co-ordinates of a point on the n-dimensional hyperplane $\omega_1 +, \ldots, + \omega_n = \omega$ and

$$\underbrace{|U| * |U| * \ldots * |U(j\omega)|}_{n} = \int_{-\infty}^{\infty} \ldots \int_{-\infty}^{\infty} |U(j\omega_1)|, \ldots, |U(j\omega_{n-1})| \, |U[j(\omega - \omega_1, \ldots, -\omega_{n-1})]| d\omega_1 \, d\omega_2, \ldots d\omega_{n-1} \tag{3.27}$$

Therefore the expression for the bound on the output frequency response magnitude characteristics of nonlinear systems can be obtained theoretically by combining (3.26), (3.27) and (3.3) to yield

$$\mathbf{Y}^B(\omega) = \sum_{n=1}^{N} \frac{1}{(2\pi)^{n-1}} |H_n[j\omega_{n1}^{\#}, j\omega_{n2}^{\#}, \ldots, j\omega_{nn}^{\#}]| \int_{-\infty}^{\infty} \ldots \int_{-\infty}^{\infty} |U(j\omega_1)|, \ldots, |U(j\omega_{n-1})| \, |U[j(\omega - \omega_1, \ldots, -\omega_{n-1})]| d\omega_1 \, d\omega_2, \ldots d\omega_{n-1} \tag{3.28}$$

Although the derivation of (3.28) is based on continuous time nonlinear systems, the conclusion for discrete time nonlinear systems is exactly the same as in the continuous time case except that in the discrete time case $U(j\omega)$ is the discrete time Fourier transformation of the system input sequence and $\mathbf{Y}^B(\omega)$ represents the bound for the magnitude frequency domain characteristic of the system output sequence.

4. ANALYSIS OF THE BOUND IN THE FREQUENCY DOMAIN CHARACTERISATION OF NONLINEAR SYSTEMS

Equation (3.28) indicates that the proposed bound for the output frequency response magnitude characteristics of nonlinear systems possesses a formation similar to the linear relationship $|\mathbf{Y}(j\omega)| = |H(j\omega)||U(j\omega)|$ because the influences of the GFRFs and the frequency characteristics of the input on this bound are decomposed in each term of the expression. This is an important feature of the new bound because it may simplify a study of the analysis and synthesis of nonlinear systems if these problems can be formulated in an analogous manner to the linear case.

In addition, this new concept also has the following properties concerning the relationship with $|\mathbf{Y}(j\omega)|$:

(i) $\mathbf{Y}^B(\omega) \ge |\mathbf{Y}(j\omega)|$

(ii) $\mathbf{Y}^B(\omega) = |\mathbf{Y}(j\omega)|$ for N = 1

(iii) $\mathbf{Y}^B(\omega) = |\mathbf{Y}(j\omega)| = 0$ if $\omega \notin \bigcup_{n=1}^{N} R_n \cup R_{-n}$

where R_n is the nonnegative frequency range produced by the nth order nonlinear output, R_{-n} is the negative frequency range produced by this output and the relationship between R_n and R_{-n} is

$$-\{R_n \setminus \{0\}\} = R_{-n} \tag{4.1}$$

with $-\{.\}$ denoting a set which possesses elements of opposite signs to those in the set $\{.\}$.

For these properties, (i) is straightforward due to the definition of $\mathbf{Y}^B(\omega)$; (ii) follows from equation (3.5) and the explanation for (iii) is given below.

It is well known that for linear systems the frequency range of the system output is the same as that of the corresponding input. Lang and Billings (1994) have shown that under the assumption that the input frequency spectrum is of the form

$$U(j\omega) = \begin{cases} U(j\omega) & \omega \in [a,b] \;\; b > a \geq 0 \\ 0 & \text{for other } \omega \geq 0 \end{cases} \tag{4.2}$$

the nonnegative frequency range R_n of the nth order nonlinear output is determined from

$$\omega = \omega_1 +, \ldots, +\omega_n \qquad \text{with } \omega_l \in [-b,-a] \text{ or } [a,b],\; l = 1,\ldots,n \tag{4.3}$$

For simplicity of explanation assume a=0 in (4.3) to yield R_n that is the nonnegative part of

$$\{\omega\!: \; \omega = \omega_1 +, \ldots, +\omega_n,\; \omega_l \in [-b,b],\; l = 1,2,\ldots,n\} \tag{4.4}$$

Considering (4.2) and a=0, (3.27) can be written as

$$\underbrace{|U| *, \ldots, * |U(j\omega)|}_{n} = \int_{-b}^{b} \cdots \int_{-b}^{b} |U(j\omega_1)|, \ldots, |U(j\omega_{n-1})| |U[j(\omega - \omega_1 -, \ldots, -\omega_{n-1})]| d\omega_1, \ldots, d\omega_{n-1} \tag{4.5}$$

The definition for R_n given by (4.4) means that if $|\omega| \notin R_n$, i.e. $\omega \notin R_n \cup R_{-n}$, then $\omega - \omega_1 -, \ldots, -\omega_{n-1} \notin [-b,b]$ in the integration process of (4.5). This implies $|U[j(\omega - \omega_1 -, \ldots, -\omega_{n-1})]| \equiv 0$ in the process and therefore

$$\underbrace{|U| *, \ldots, * |U(j\omega)|}_{n} = 0 \tag{4.6}$$

and

$$Y_n^B(\omega) = \frac{1}{(2\pi)^{(n-1)}} |H_n(j\omega_{n1}^{\#}, \ldots, j\omega_{nn}^{\#})| \underbrace{|U| *, \ldots, * |U(j\omega)|}_{n} = 0 \tag{4.7}$$

Thus, it is quite clear that if

$$\omega \notin \bigcup_{n=1}^{N} R_n \cup R_{-n} \tag{4.8}$$

then

$$Y_n^B(\omega) = 0 \qquad \text{for n=1,2,...N} \tag{4.9}$$

and

$$\mathbf{Y}^B(\omega) = \sum_{n=1}^{N} Y_n^B(\omega) = 0 \tag{4.10}$$

Furthermore combining (4.10) and

$$\mathbf{Y}^B(\omega) \geq |\mathbf{Y}(j\omega)| \geq 0 \tag{4.11}$$

gives

$$\mathbf{Y}^B(\omega) = |\mathbf{Y}(j\omega)| = 0 \tag{4.12}$$

that is (iii) holds. For the case $a \neq 0$, this can also be proved in a similar way.

These properties especially properties (ii) and (iii) indicate that $\mathbf{Y}^B(\omega)$ is not a conservative bound for $|\mathbf{Y}(j\omega)|$. In fact as shown in the following simulation examples, this bound can sometimes even be applied to evaluate the trend in the variation of $|\mathbf{Y}(j\omega)|$.

5. PRACTICAL COMPUTATION OF THE BOUND

5.1 The evaluation of $|H_n(j\omega^{\#}_{n1},\dots,j\omega^{\#}_{nn})|$

Clearly the expression (3.28) is only of theoretical significance. To calculate $\mathbf{Y}^B(\omega)$ practically methods for evaluating $|H_n(j\omega^{\#}_{n1},\dots,j\omega^{\#}_{nn})|$ and $\underbrace{|U|*,\dots,*|U(j\omega)|}_{n}$ still need to be developed. Generally $|H_n(j\omega^{\#}_{n1},\dots,j\omega^{\#}_{nn})|$ is hard to determine precisely because the exact position of the point $\{\omega^{\#}_{n1},\dots,\omega^{\#}_{nn}\}$ on the n-dimensional hyperplane $\omega = \omega_1+,\dots,+\omega_n$ is unknown. However in practice $|H_n(j\omega^{\#}_{n1},\dots,j\omega^{\#}_{nn})|$ in (3.28) can be replaced by $|H_n(j\omega_1,\dots,j\omega_n)|^B_\omega$, a bound for $|H_n(j\omega_1,\dots,j\omega_n)|$ with $\omega_1,\dots,\omega_n$ satisfying the constraint $\omega = \omega_1+,\dots,+\omega_n$ to evaluate

$$\overline{\mathbf{Y}}^B(\omega) = \sum_{n=1}^{N} \frac{1}{(2\pi)^{(n-1)}} |H_n(j\omega_1,\dots,j\omega_n)|^B_\omega \underbrace{|U|*,\dots,*|U(j\omega)|}_{n} \tag{5.1}$$

giving an approximate value of the theoretical result $\mathbf{Y}^B(\omega)$. Obviously $\overline{\mathbf{Y}}^B(\omega) \geq \mathbf{Y}^B(\omega)$ and this also possesses the properties analysed in the last section. Based on this idea and the algorithm proposed in the next section for the computation of $\underbrace{|U|*,\dots,*|U(j\omega)|}_{n}$, procedures for the practical computation of the bound for nonlinear systems which can be described by the polynomial NARX model have been developed and will be presented in Part II of this paper.

5.2 Algorithm for the computation of $\underbrace{|U|*,\ldots,*|U(j\omega)|}_{n}$

In the following, an algorithm for the computation of the n-dimensional convolution integral for $|U(j\omega)|$ given by (3.27) is proposed which can be easily applied in practice.

Denote

$$\overline{U}_n(\omega) = \underbrace{|U|*,\ldots,*|U(j\omega)|}_{n} \tag{5.2}$$

and examine the Fourier transformation of $\overline{U}_n(\omega)$ to give

$$F[\overline{U}_n(\omega)] = F\ [\underbrace{|U|*,\ldots,*|U(j\omega)|}_{n}] = F^n[|U(j\omega)|] \tag{5.3}$$

Let $U_d(j\overline{\omega})$ be the discrete time Fourier transformation of a sampling sequence of u(t) with the sampling period T, then according to the relationship between the frequency characteristics of a continuous signal and the corresponding sampling sequence (Glenn and Fred 1994) for an appropriate sampling period T

$$U_d(j\overline{\omega}) = U_d(jT\omega) = \tfrac{1}{T}U(j\omega) \tag{5.4}$$

Substituting (5.4) into (5.3) yields

$$F[\overline{U}_n(\omega)] = F^n[T|U_d(jT\omega)|] = T^n\ F^n[|U_d(jT\omega)|] \tag{5.5}$$

Assume that $|U_d(j\omega T)|$ has been obtained in the form of

$$\left|U_d(j\frac{2\pi}{M}l)\right| \quad ,l = -(M/2-1),-(M/2-2),\ldots,-1,0,1,\ldots,M/2 \tag{5.6}$$

from the M (an even number) sampled values of u(t) by using the FFT and denote the result of the Fourier transformation of the discrete data in (5.6) as $F[|U_d(l)|]$. According to Glenn and Fred (1994) it is known that for a sufficiently large M

$$F[\overline{U}_n(\omega)] = T^n\ F^n[|U_d(j\omega T)|] = T^n(2\pi/TM)^n F^n[|U_d(l)|]\Big|_{\omega_d=\frac{2\pi}{TM}\omega_c} \tag{5.7}$$

In (5.7), ω_d and ω_c represent the frequencies in the Fourier transformation results $F[|U_d(l)|]$ as well as $F[|U_d(jT\omega)|$ and $F[\overline{U}_n(\omega)]$ respectively.

Because for a time series $x(n)$,

$$F[x(n-n_0)] = F[x(n)]e^{-j\omega_d n_0}$$

$F^n[|U_d(l)|]$ in (5.7) can be written as

$$F^n[|U_d(l)|] = \{F[|U_d[l-(M/2-1)]|]e^{j\omega_d(M/2-1)}\}^n = F^n[|U_d[l-(M/2-1)]|]e^{jn\omega_d(M/2-1)} \tag{5.8}$$

From the definition of the Fourier transformation for discrete time series,

$$F[|U_d[l-(M/2-1)]|] = \left|U_d[-j\frac{2\pi}{M}(\frac{M}{2}-1)]\right| + \left|U_d[-j\frac{2\pi}{M}(\frac{M}{2}-2)]\right|e^{-j\omega_d} +,\dots,+ \left|U_d[-j\frac{2\pi}{M}0]\right|e^{-j(\frac{M}{2}-1)\omega_d}$$
$$+,\dots,+\left|U_d[j\frac{2\pi}{M}\frac{M}{2}]\right|e^{-j\omega_d(M-1)}$$

$$= \tilde{U}(0) + \tilde{U}(1)e^{-j\omega_d} +,\dots,+ \tilde{U}(\tfrac{M}{2}-1)e^{-j(\frac{M}{2}-1)\omega_d} +,\dots,+ \tilde{U}(M-1)e^{-j\omega_d(M-1)} \tag{5.9}$$

where

$$\begin{cases} \tilde{U}(0) = \left|U_d[-j\frac{2\pi}{M}(\frac{M}{2}-1)]\right| \\ \tilde{U}(1) = \left|U_d[-j\frac{2\pi}{M}(\frac{M}{2}-2)]\right| \\ \vdots \\ \tilde{U}(\frac{M}{2}-1) = \left|U_d[j\frac{2\pi}{M}0]\right| \\ \vdots \\ \tilde{U}(M-1) = \left|U_d[j\frac{2\pi}{M}\frac{M}{2}]\right| \end{cases} \tag{5.10}$$

Therefore

$$F^n[|U_d(l)|] = [\tilde{U}(0) + \tilde{U}(1)e^{-j\omega_d} +,\dots,+ \tilde{U}(\tfrac{M}{2}-1)e^{-j(\frac{M}{2}-1)\omega_d} +,\dots,+ \tilde{U}(M-1)e^{-j\omega_d(M-1)}]^n e^{jn\omega_d(\frac{M}{2}-1)}$$

$$= \text{Conv}\{\underbrace{[\tilde{U}(0),\dots,\tilde{U}(M-1)],\dots,[\tilde{U}(0),\dots,\tilde{U}(M-1)]}_{n}\}\begin{bmatrix} 1 \\ e^{-j\omega_d} \\ \vdots \\ \vdots \\ e^{-j\omega_d n(M-1)} \end{bmatrix} e^{jn\omega_d(\frac{M}{2}-1)}$$

$$= \{\tilde{\tilde{U}}(0) + \tilde{\tilde{U}}(1)e^{-j\omega_d} +,..,+ \tilde{\tilde{U}}[n(M-1)]e^{-j\omega_d n(M-1)}\}e^{jn\omega_d(\frac{M}{2}-1)}$$

$$= \tilde{\tilde{U}}(0)e^{jn\omega_d(\frac{M}{2}-1)} + \tilde{\tilde{U}}(1)e^{j\omega_d[n(\frac{M}{2}-1)-1]} +,..,+ \tilde{\tilde{U}}[n(M-1)]e^{-j\omega_d n\frac{M}{2}} \tag{5.11}$$

where $Conv\{\overbrace{x,\dots x}^{n}\}$ denotes the n-dimensional convolution for a vector x, and

$$\{\tilde{\tilde{U}}(0),\dots,\tilde{\tilde{U}}[n(M-1)]\} = \text{Conv}\{\underbrace{[\tilde{U}(0),\dots,\tilde{U}(M-1)],\dots,[\tilde{U}(0),\dots,\tilde{U}(M-1)]}_{n}\} \tag{5.12}$$

Combining (5.7) and (5.11) yields

$$F[\overline{U}_n(\omega)] = T^n\left(\frac{2\pi}{MT}\right)^n F^n[|U_d(l)|]\Big|_{\omega_d=\frac{2\pi}{MT}\omega_c}$$

$$= T^n\left(\frac{2\pi}{MT}\right)^n \{\tilde{\tilde{U}}(0)e^{jn\omega_d(\frac{M}{2}-1)} + \tilde{\tilde{U}}(1)e^{j\omega_d[n(\frac{M}{2}-1)-1]} +,..,+ \tilde{\tilde{U}}[n(M-1)]e^{-j\omega_d n\frac{M}{2}}\}\Big|_{\omega_d=\frac{2\pi}{MT}\omega_c} \tag{5.13}$$

Denote $\{\overline{U}_n(l)\}$ as a sampling sequence of $\overline{U}_n(\omega)$ with the sampling interval $2\pi/MT$ so that according to Glenn and Fred (1994)

$$F[\overline{U}_n(l)] = \frac{1}{2\pi/MT} F[\overline{U}_n(\omega)]\Big|_{\omega_c = \frac{MT}{2\pi}\omega_d} = T(2\pi/M)^{n-1}\{\tilde{\tilde{U}}(0)e^{jn\omega_d(\frac{M}{2}-1)} + \tilde{\tilde{U}}(1)e^{j\omega_d[n(\frac{M}{2}-1)-1]} +$$

$$,..,+\tilde{\tilde{U}}[n(M/2-1)]e^{-j\omega_d 0}+,\ldots,+\tilde{\tilde{U}}[n(M-1)]e^{-j\omega_d n\frac{M}{2}}\}$$

(5.14)

which implies that

$$\begin{cases} \overline{U}_n[-n\left(\frac{M}{2}-1\right)\frac{2\pi}{MT}] = T\tilde{\tilde{U}}(0)\left(\frac{2\pi}{M}\right)^{n-1} \\ \overline{U}_n[(-n\left(\frac{M}{2}-1\right)+1)\frac{2\pi}{MT}] = T\tilde{\tilde{U}}(1)\left(\frac{2\pi}{M}\right)^{n-1} \\ \vdots \\ \overline{U}_n[0\frac{2\pi}{MT}] = T\tilde{\tilde{U}}[n\left(\frac{M}{2}-1\right)]\left(\frac{2\pi}{M}\right)^{n-1} \\ \vdots \\ \overline{U}_n[n\left(\frac{M}{2}\right)\frac{2\pi}{MT}] = T\tilde{\tilde{U}}[n(M-1)]\left(\frac{2\pi}{M}\right)^{n-1} \end{cases}$$

(5.15)

Thus combining (5.10), (5.12), (5.15), and (5.2) gives the algorithm for calculating the n-dimensional convolution integral for $|U(j\omega)|$ at the points

$$\omega = i\frac{2\pi}{MT}, \quad i = -n(\frac{M}{2}-1),\ldots,0,\ldots,n\frac{M}{2} \tag{5.16}$$

as follows

$$\begin{cases} \underbrace{|U|*,\ldots,*\left|U[j(\frac{2\pi}{MT}i)]\right|}_{n} = \overline{U}_n[i\frac{2\pi}{MT}] = T\tilde{\tilde{U}}[i+(\frac{M}{2}-1)n]\left(\frac{2\pi}{M}\right)^{n-1} \qquad i = -n(\frac{M}{2}-1),\ldots,0,\ldots,n\frac{M}{2} \\ \{\tilde{\tilde{U}}(0),\ldots,\tilde{\tilde{U}}[n(M-1)]\} = \text{Conv}\underbrace{\{[\tilde{U}(0),\ldots,\tilde{U}(M-1)],\ldots,[\tilde{U}(0),\ldots,\tilde{U}(M-1)]\}}_{n} \\ \tilde{U}(i) = \left|U_d[j\frac{2\pi}{M}(i-\frac{M}{2}+1)]\right|, \quad i = 0,1,\ldots,M-1 \end{cases}$$

(5.17)

It should be noted that the above algorithm has been obtained on the assumption that no aliasing phenomena appear in either the input or output of the system because of sampling. This implies that the sampling period T for u(t) must be chosen appropriately to satisfy this requirement. In addition (5.7) and (5.14) require a sufficiently large M and hence an appropriate length M of the sampled data must be used to compute $\left|U_d(j\frac{2\pi}{M}l)\right|$, $l = -(\frac{M}{2}-1),\ldots,0,\ldots,\frac{M}{2}$.

If the system is a discrete time system then $U_d(j\omega) = U(j\omega)$ and the algorithm is exactly the same as (5.17) except that T in (5.17) is taken as 1.

Clearly the algorithm (5.17) can easily be evaluated up to arbitrary order nonlinearities. This indicates that the algorithm together with the method for evaluating $|H_n(j\omega^{\#}_{n1},\ldots,j\omega^{\#}_{nn})|$ discussed in Section 5.1 can be applied to carry out the analysis of nonlinear systems with finite but arbitrary order nonlinearities to evaluate the new concept $\mathbf{Y}^B(\omega)$ or $\overline{\mathbf{Y}}^B(\omega)$.

6. EXAMPLES

In this section two simple examples are given to illustrate the new bound . The emphasis is upon illustrating the properties analysed in Section 4 and the effectiveness of the algorithm proposed in Section 5.2.

Example 1

Consider a nonlinear system

$$y(t) = H(D)\alpha_3 u^3(t) \tag{6.1}$$

where D is the differential operator, $\alpha_3 = 1$, and

$$H(D) = \frac{w_n^2}{D^2 + 2\xi w_n D + w_n^2} \tag{6.2}$$

with $w_n = 10\pi/3$ and $\xi = 0.2$. The frequency characteristic of the input is shown in Fig.3 and this implies

$$u(t) = \frac{1}{2\pi}\int_{-\infty}^{\infty} U(j\omega)\, e^{j\omega t}\, d\omega = \frac{1}{2\pi}\int_{-5}^{-1} U(j\omega)\, e^{j\omega t}\, d\omega + \frac{1}{2\pi}\int_{1}^{5} U(j\omega)\, e^{j\omega t}\, d\omega$$

$$= \frac{1}{2\pi}[\int_{-5}^{-3}\frac{1}{2}\, e^{j\omega t}\, d\omega + \int_{-3}^{-2} -\frac{1}{2}\, e^{j\omega t}\, d\omega + \int_{-2}^{-1}\frac{1}{2}\, e^{j\omega t}\, d\omega + \int_{3}^{5}\frac{1}{2}\, e^{j\omega t}\, d\omega + \int_{2}^{3} -\frac{1}{2}\, e^{j\omega t}\, d\omega + \int_{1}^{2}\frac{1}{2}\, e^{j\omega t}\, d\omega$$

$$= \frac{2(\sin 2t - \sin 3t) + \sin 5t - \sin t}{2\pi\, t} \tag{6.3}$$

with

$$u(0) = \frac{4\cos 2t - 6\cos 3t + 5\cos 5t - \cos t}{2\pi}\Big|_{t=0} = \frac{1}{\pi}$$

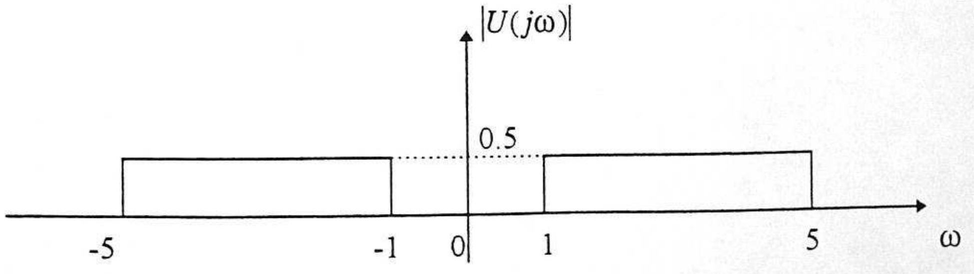

Fig.3 (a)

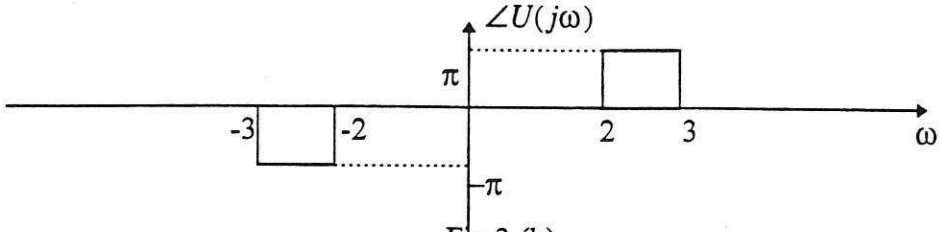

Fig.3 (b)

Fig.3 The frequency characteristic of u(t) in Example 1

The GFRFs of the system can easily be obtained as

$$\begin{cases} H_3(j\omega_1, j\omega_2, j\omega_3) = \alpha_3 H[j(\omega_1+\omega_2+\omega_3)] \\ \qquad = \dfrac{\alpha_3 w_n^2}{[j(\omega_1+\omega_2+\omega_3)]^2 + 2\xi w_n[j(\omega_1+\omega_2+\omega_3)] + w_n^2} \\ H_n(j\omega_1,\ldots,j\omega_n) = 0, \quad \text{for } n = 1,2, \text{and } n \ge 4 \end{cases} \tag{6.4}$$

From (3.28) and (6.4) the bound for the magnitude frequency domain characteristic of the system output can be written as

$$\mathbf{Y}^B(\omega) = \sum_{n=1}^{3} \frac{1}{(2\pi)^{n-1}} \left|H_n(j\omega_{n1}^{\#},\ldots,j\omega_{nn}^{\#})\right| \underbrace{|U|*\cdots*|U(j\omega)|}_{n}$$

$$= \frac{1}{(2\pi)^2}\left|H_3(j\omega_{31}^{\#}, j\omega_{32}^{\#}, j\omega_{33}^{\#})\right| |U|*|U|*|U(j\omega)| = \frac{\alpha_3}{(2\pi)^2}\left|H(j\omega)\right| |U|*|U|*|U(j\omega)|$$

$$= \frac{1}{(2\pi)^2}\left|\frac{(10\pi/3)^2}{(j\omega)^2 + 2\times 0.2\times 10\pi/3\, j\omega + (10\pi/3)^2}\right| \overline{U}_3(\omega) \tag{6.5}$$

By using the algorithm proposed in Section 5.2 with M=2000 and T=0.2, first obtain

$$\left|U_d[j\frac{2\pi}{M}(i-\frac{M}{2}+1)]\right| \qquad \text{for } i = 0,1,\ldots,M-1,$$

the discrete Fourier transformation of M sampled values of u(t) with the sampling period T=0.2 as shown in Fig. 4. Then calculate $\overline{U}_3(\omega) = |U|*|U|*|U(j\omega)|$ from (5.17) giving

$$\overline{U}_3(i\frac{2\pi}{2000\times 0.2}) \quad \text{for } i = -3(\frac{2000}{2}-1),\ldots,0,\ldots,3\frac{2000}{2}$$

as shown in Fig.5. From (6.5) $\mathbf{Y}^B(\omega)$ for the system under the excitation of u(t) is then obtained and shown in Fig.6.

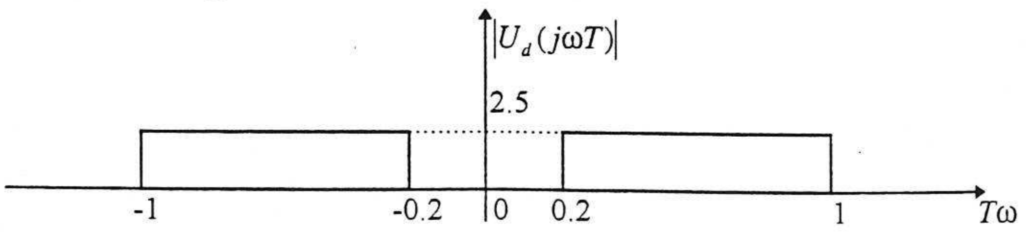

Fig.4 The magnitude characteristic of the discrete time Fourier transformation for the sampled values of u(t) with T=0.2

To illustrate the relationship between $\mathbf{Y}^B(\omega)$ and $|\mathbf{Y}(j\omega)|$ in this particular case, $y(kT_s)\big|_{T_s=0.1}$ $k = 0,\pm1,\pm2,\ldots$ are determined from the system output $y(t)$ which was obtained by continuous simulation of the system equation (6.1) with u(t) given by (6.3) . The discrete time Fourier transformation was then computed using an FFT algorithm for the frequencies $-\frac{1999}{2000}\pi,\ldots,0,\ldots,\frac{2000}{2000}\pi$. The transformation results were then multiplied by $T_s = 0.1$, and $|Y(j\omega)|$ was determined for $\omega = -\frac{1999}{2000T_s}\pi\big|_{T_s=0.1},\ldots,0,\ldots,\frac{2000}{2000T_s}\pi\big|_{T_s=0.1}$. Fig.6 shows a comparison of $|\mathbf{Y}(j\omega)|$ with the computed bound $\mathbf{Y}^B(\omega)$.

The results in Fig.6 indicate that

$$\mathbf{Y}^B(\omega) = |\mathbf{Y}(j\omega)| = 0 \qquad \text{when} \qquad |\omega| \geq 15 \tag{6.6}$$

which verifies the third property of $\mathbf{Y}^B(\omega)$ analysed in Section 4 because in this case applying the algorithm for computing R_n in Lang and Billings (1994) yields

$$\bigcup_{n=1}^{N} R_n \cup R_{-n} = R_3 \cup R_{-3} = [0\ ,\ 15] \cup [-15\ ,\ 0) = [-15,\ +15]$$

The results also illustrate the practicability of the new concept since it can be seen from Fig.6 (especially Fig. 6 (b)) that the overall trend in the variation of $|\mathbf{Y}(j\omega)|$ is basically reflected by the result obtained $\mathbf{Y}^B(\omega)$.

Example 2

Consider a discrete time nonlinear system

$$y(k) = \frac{q^{-d}B(q^{-1})}{A(q^{-1})}[\alpha_1 u(k) + \alpha_2 u^2(k)] \tag{6.7}$$

where q^{-1} is the backward shift operator and

$$A(q^{-1}) = 1 - 0.6q^{-1} + 0.08q^{-2}$$

$$B(q^{-1}) = 1 - 0.5q^{-1},\quad d = 1,\quad \alpha_1 = 1,\quad \alpha_2 = -1..5$$

The input sequence u(k) is

$$u(k) = \frac{1}{2\pi}\frac{\sin(5kT_s) - \sin(kT_s)}{kT_s}\bigg|_{T_s=0.2}, \qquad k = 0,\pm1,\pm2,\ldots \tag{6.8}$$

with

$$u(0) = \frac{1}{2\pi}(5\cos 5t - \cos t)\big|_{t=0} = \frac{2}{\pi}$$

The magnitude frequency domain characteristic of u(k) is of the form shown in Fig.7.

The GFRFs of the system can easily be obtained as

$$\begin{cases} H_1(j\omega_1) = \alpha_1 H(e^{-j\omega_1}) = H(e^{-j\omega_1}) \\ H_2(j\omega_1, j\omega_2) = \alpha_2 H(e^{-j(\omega_1+\omega_2)}) = -1.5H(e^{-j(\omega_1+\omega_2)}) \\ H_n(j\omega_1,\ldots,j\omega_n) = 0 \qquad \text{for } n \geq 3 \end{cases} \tag{6.9}$$

where

$$H(e^{-j\omega}) = \frac{e^{-j\omega}B(e^{-j\omega})}{A(e^{-j\omega})}$$

From (3.28) and (6.9), the bound for the magnitude frequency domain characteristic of the output of the system (6.7) can be written as

$$\begin{aligned} \mathbf{Y}^B(\omega) &= \sum_{n=1}^{2} \frac{1}{(2\pi)^{n-1}} \left|H(j\omega_{n1}^{\#},\ldots,j\omega_{nn}^{\#})\right| \underbrace{|U|*\cdots*|U(j\omega)|}_{n} \\ &= \left|H_1(j\omega\ )\right|\left|U(j\omega)\right| + \frac{1}{2\pi}\left|H_2(j\omega_{21}^{\#}, j\omega_{22}^{\#})\right||U|*|U(j\omega)| \\ &= \left|H(e^{-j\omega})\right|\left|U(j\omega)\right| + \frac{1.5}{2\pi}\left|H(e^{-j\omega})\right||U|*|U(j\omega)| = \left|H(e^{-j\omega})\right|\left[\left|U(j\omega)\right| + \frac{1.5}{2\pi}|U|*|U(j\omega)|\right] \end{aligned} \tag{6.10}$$

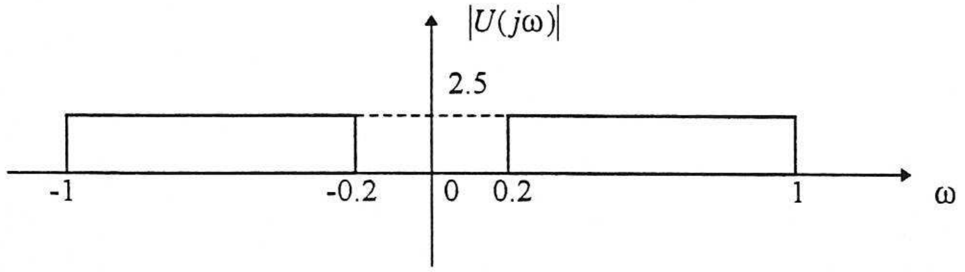

Fig.7. The magnitude frequency characteristic of u(k) in Example 2

By using the algorithm proposed in Section 5.2 with M=2000, $T = 1$ and $|U_d(j\omega)| = |U(j\omega)|$ (because a discrete time system is considered in this example), $|U|*|U(j\omega)|$ for $\omega = -2\times\frac{999}{1000}\pi,\ldots,0,\ldots,2\times\frac{1000}{1000}\pi$ is computed and shown in Fig.8 for the frequency range $\omega \in [-\pi,\pi]$. Combining $|U|*|U(j\omega)|$, $|U(j\omega)|$ and $|H(e^{-j\omega})|$ for $\omega = -\frac{999}{1000}\pi,\ldots,0,\ldots,\frac{1000}{1000}\pi$ as indicated in (6.10) yields $\mathbf{Y}^B(\omega)$ at these frequencies as shown in Fig.9.

To make a comparison between $\mathbf{Y}^B(\omega)$ and $|\mathbf{Y}(j\omega)|$ in this case, $y(k), k = 0,\pm1,\pm2,\ldots$ were computed from (6.7) and the output frequency characteristic $\mathbf{Y}(j\omega)$ for $\omega = -\frac{999}{1000}\pi,\ldots,0,\ldots,\frac{1000}{1000}\pi$ was obtained by applying the FFT to $y(k)$ for $k = -999,\ldots,0,\ldots,1000$ giving the corresponding $|\mathbf{Y}(j\omega)|$ at these frequencies. This is shown in Fig.9 for comparison.

The results in Fig.9 indicate that

$$\mathbf{Y}^B(\omega) = |\mathbf{Y}(j\omega)| = 0 \qquad \text{when} \quad \pi \geq |\omega| \geq 2$$

which is also consistent with the property of $\mathbf{Y}^B(\omega)$ analysed in Section 4 since in this example

$$\bigcup_{n=1}^{N} R_n \cup R_{-n} = \bigcup_{n=1}^{2} R_n \cup R_{-n} = [-1, \ -0.2] \cup [0.2, \ 1] \cup [-2, \ 2] = [-2, \ 2]$$

Fig.9 also shows that the trend in the variation of $|\mathbf{Y}(j\omega)|$ is reflected by $\mathbf{Y}^B(\omega)$.

7. CONCLUSIONS

A new bound has been derived for the output magnitude frequency domain characteristics of a wide class of nonlinear systems. Most of the analysis and synthesis methods which have been developed in the frequency domain for linear systems are based on the magnitude characteristics of the system output and the new bound provides a basis for extending these results to the nonlinear case. Interpretation of the new bound in terms of the generalised frequency response functions and characteristics of the input has been included and general methods for the practical computation of the bound have also been developed.

Part II of this paper will consider the practical computation of the bound for the class of nonlinear systems which can be described by the polynomial NARX model.

Acknowledges

SAB gratefully acknowledges support from the UK EPSRC for part of this work under grant ref. GR/J05149 and ZQL acknowledges the support provided by Sheffield University under the scholarship scheme..

REFERENCES

Bedrosian, E. and Rice, S.O., 1971, The output properties of Volterra systems driven by harmonic and gaussian inputs, Proc IEEE, Vol.59, pp1688-1707.

Billings, S.A. and Tsang, K.M., 1989(a), Spectral analysis for nonlinear systems, Part I: Parametric nonlinear spectral analysis, Mechanical Systems and Signal Processing, 3, 319-339.

Billings, S.A. and Tsang, K.M., 1989(b), Spectral analysis for nonlinear systems, Part II: Interpretation of nonlinear frequency response functions, Mechanical Systems and Signal Processing, 3, 341-359.

Billings, S.A., Tsang, K.M., and G.R. Tomlinson, 1990, Spectral analysis for nonlinear systems, Part III: Case study examples, Mechanical Systems and Signal Processing, 4, 3-21.

Billings, S.A. and Peyton Jones, J.C., 1990, Mapping nonlinear integro-differential equation into the frequency domain. Int. J. Control, 52(4), 863-879.

Billings, S.A. and Yusof, M.I., 1994, Decomposition of generalised frequency response functions for nonlinear systems using symbolic computation. submitted for publication.

Bussgang, J.J., Ehrman, L., and Garham, J.W., 1974, Analysis of nonlinear systems with multiple inputs, Proceedings of the IEEE, 62, 1088-1119.

Chen, S., and Billings, S.A., 1989, Representation of nonlinear systems: the NARMAX model. Int. J. Control, 49, 1013-1032.

Cho, Y.S., Kim, S.D., Hixson, E.L. and Powers, E.J., 1992, A digital technique to estimate second order distortion using higher order coherence spectra. IEEE Trans. on Acoustic Speech and Signal Processing, 40(5), 1029-1040.

Glenn Z. and Fred J. T., 1994, Advanced digital signal processing. Marcel Dekker, Inc., pp87-102.

James G. and James R. C., 1959, Mathematics dictionary. D. Van Nostrand Company, INC, Page 248.

Lang Zi-Qiang and Billings, S.A., 1994, Output frequency characteristics of nonlinear systems. submitted for publication.

Kim, K.I. and Powers, E.J., 1988, A digital method of modelling quadratically nonlinear systems with a general random input. IEEE Trans. on Acoustic , Speech ,and Signal Processing, 36, 1758-1769.

Peyton Jones, J.C. and Billings, S.A., 1989, A recursive algorithm for computing the frequency response of a class of nonlinear difference equation models, Int. J. Control, 50(5), 1925-1949.

Powers, E. J. and Miksad R.W., 1987, Polyspectral measurement and analysis of nonlinear wave interactions, Proc. Symp. on Nonlinear Wave Interactions in Fluids, pp9-16.

Spiegel Murray.R., 1974, Theory and problems of advanced calculus. S1 (Metric) Edition, Schaums Outline Series, McGraw-Hill Book Company, Chapter 10, pp198-199.

Vinh, T., Chouychai, T., Liu, H., and Djouder, m., 1987, Second order transfer function: Computation and physical interpretation. 5th IMAC, London.

Worden, K., Stansby, P.K., Tomlinson, G.R., and Billings, S.A., 1994, Identification of nonlinear wave forces. Journal of Fluids and Structures, 8, 19-71.

Zhang, H., Billings, S.A. and Zhu, Q.M., 1993, Frequency response functions for nonlinear rational models, Int. J. Control (to appear).

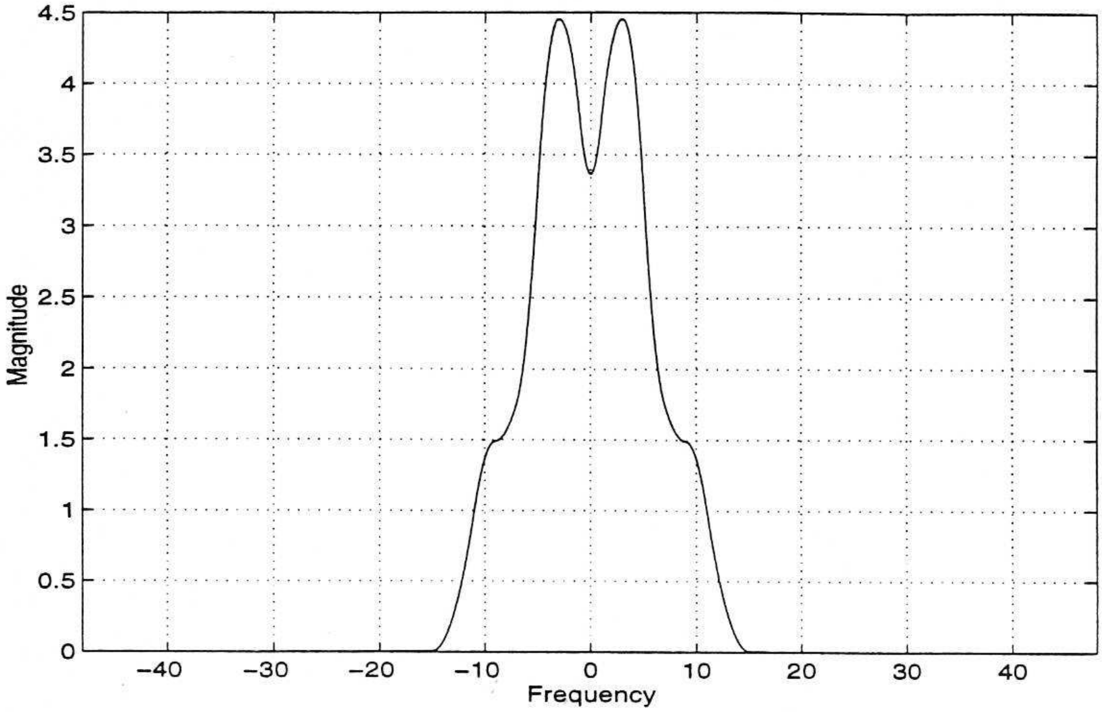

Fig.5 The result of 3-dimensional convolution integration for the magnitude of $U(j\omega)$ in Example 1

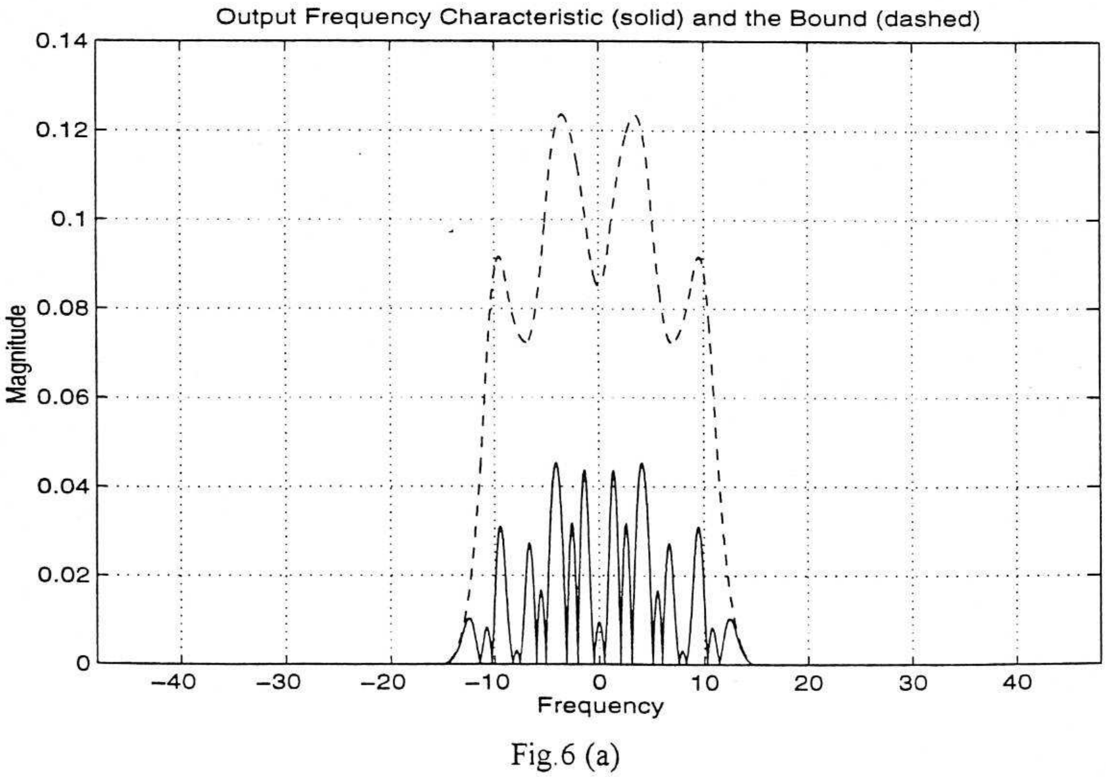

Fig.6 (a)

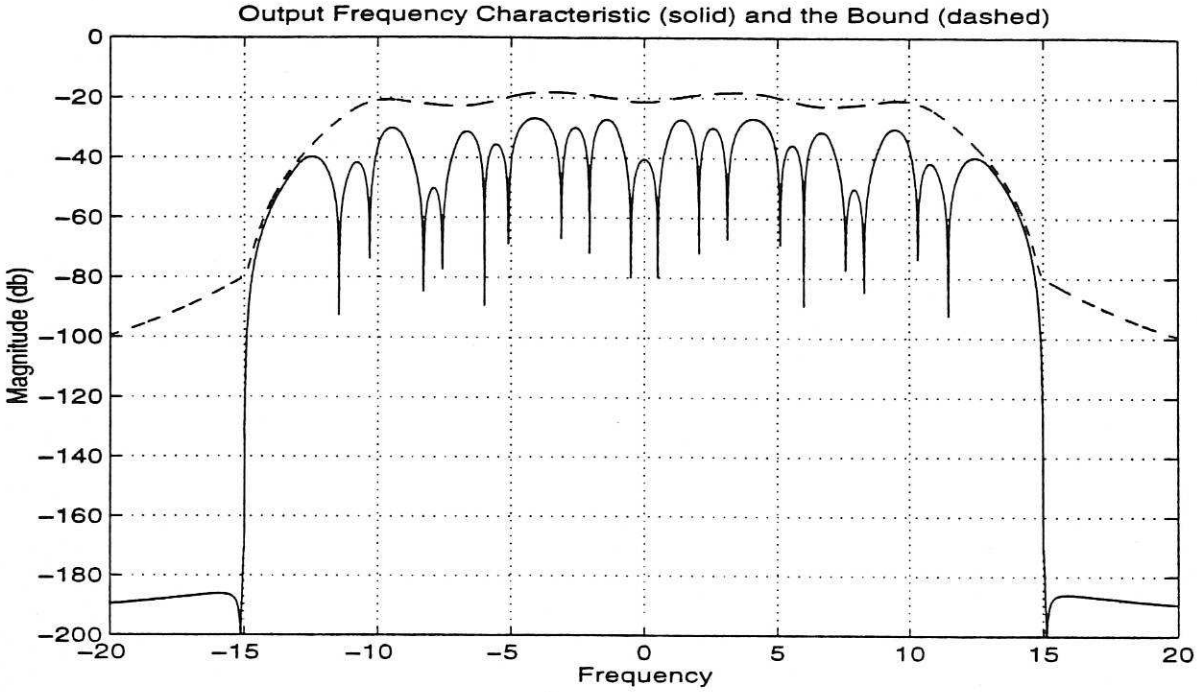

Fig.6 (b)

Fig.6 . The comparision between the magnitude characteristic of the output frequency response and the bound $\mathbf{Y}^{B}(\omega)$ in Example 1.

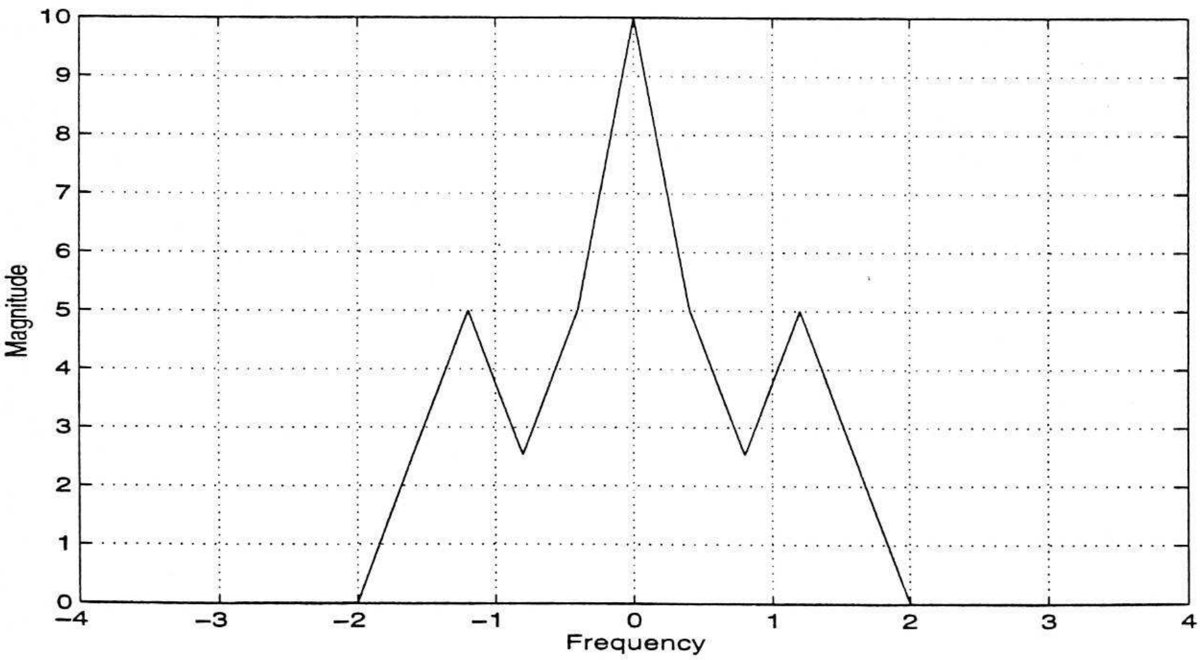

Fig.8. The result of 2-dimensional convolution integration for the magnitude of $U(j\omega)$ in Example 2.

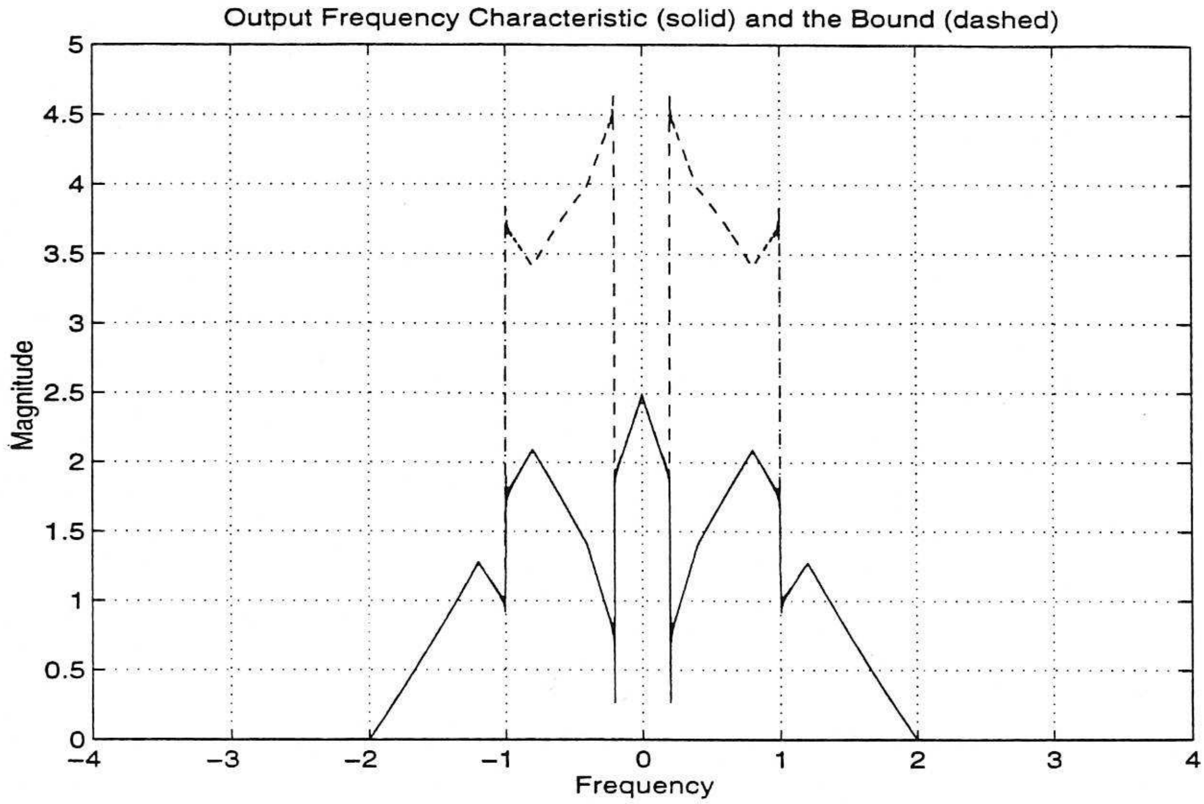

Fig.9 (a)

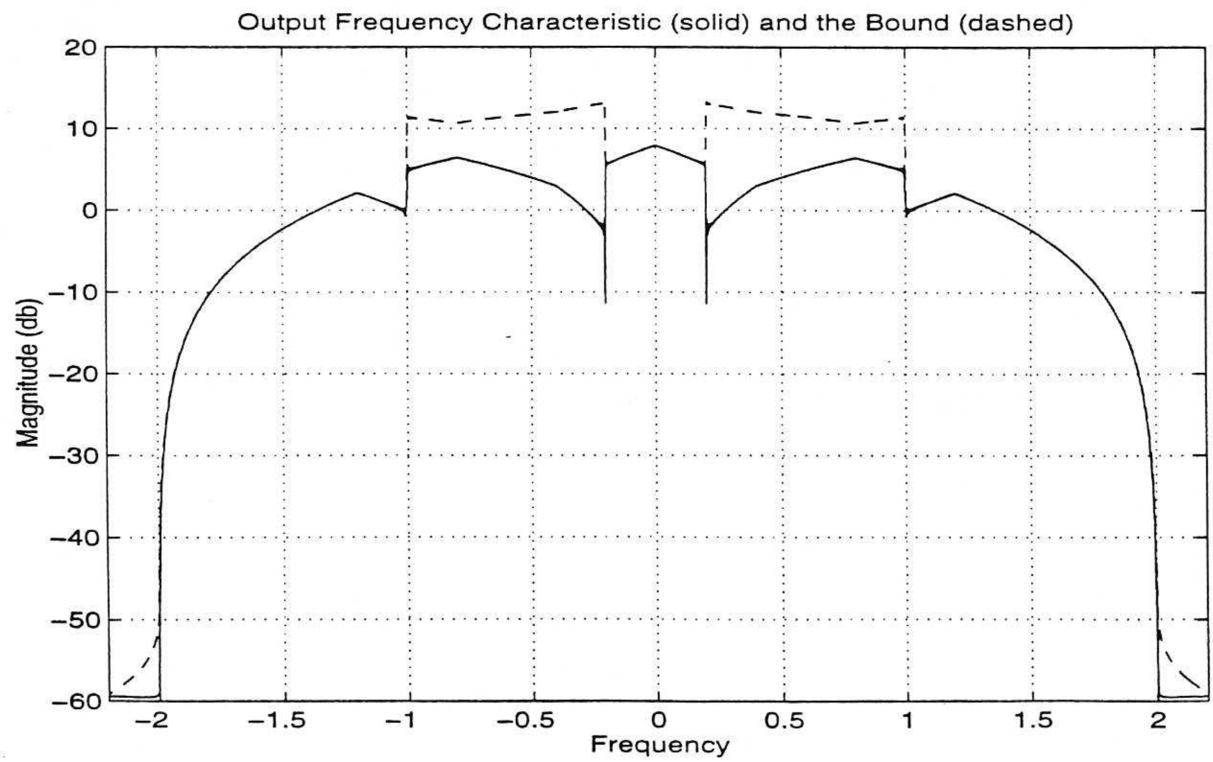

Fig.9 (b)

Fig.9 The comparision between the magnitude characteristic of the output frequency response and the bound $\mathbf{Y}^B(\omega)$ in Example 2.